

# Nuclear fission dynamics within a generalized Langevin approach

V. M. Kolomietz\* and S. V. Radionov†

*Institute for Nuclear Research, 03680 Kiev, Ukraine*

(Received 13 December 2008; revised manuscript received 30 May 2009; published 17 August 2009)

Within the generalized (non-Markovian) multidimensional Langevin approach, the time and energy characteristics of symmetric fission of highly excited heavy nuclei are studied. In two-dimensional space of the collective deformation parameters, it is considered a nuclear descent from the top of the fission barrier to the scission point. The distributions of descent times and total kinetic energy of fission fragments are calculated as functions of memory time, measuring the relative size of memory effects in the collective dynamics. We found that the peculiarities of the non-Markovian dynamics at fairly large values of the memory time are reflected in the saturation of the mean time of motion from the saddle to scission with the growth of the strength of memory effects in the system.

DOI: [10.1103/PhysRevC.80.024308](https://doi.org/10.1103/PhysRevC.80.024308)

PACS number(s): 24.75.+i, 21.60.Ev, 24.30.Cz, 24.60.Ky

## I. INTRODUCTION

Nuclear large-scale dynamics (nuclear fission, heavy-ion collisions, etc.) is a good probe for the investigation of the complex time evolution of finite Fermi systems. The conceptual question here is how collective modes of motion appear in a system with many degrees of freedom and how they interact with all other intrinsic modes. Nuclear collective dynamics can be studied by using the concept of macroscopic motion for a few collective degrees of freedom, which are chosen to describe the gross properties of the nucleus [1–3]. Such approaches are acceptable for the slow collective motion where the fast intrinsic degrees of freedom exert forces on the collective variables. The crucial point there is the separation of the total energy of the system into potential energy, collective kinetic energy, and excitation energy obtained by dissipation. Moreover, the dissipation of collective motion implies fluctuations in the corresponding collective variables, as follows from the fluctuation-dissipation theorem [4].

Dissipation of the nuclear collective energy reveals itself, for instance, in the nonzero contribution of the internucleonic collisions to the widths of the nuclear giant multipole resonances. On the other hand, the experimental observation of the finite variance of the kinetic energy of the fission fragments gives rise to the fact that fluctuations also have to be associated with the collective variables. Both the dissipation and the fluctuations can be described by introducing friction and random forces, which are related to each other through the fluctuation-dissipation theorem. In this respect, the Fokker-Planck or Langevin approaches are suitable for the study of the nuclear large-scale dynamics (see Refs. [5–7] and references therein). In general, basic equations of motion for the macroscopic parameters, describing the complex dynamics of many-body systems like nuclei, have non-Markovian structure. One of the first considerations of memory (non-Markovian) effects for classical liquids can be found in Ref. [8]. For the collective dynamics in atomic nuclei, memory effects have

been investigated earlier within different approaches, such as the dissipative diabatic model [9–11], the linear response theory [3,12], and the fluid dynamic approach [13–16]. Thus, in Refs. [5] and [17], within the one-dimensional generalized Langevin approach, it was found that memory effects in collective dynamics enlarge the fission rate and accelerate a nuclear descent from the fission barrier (see also Ref. [18]). In this respect, it will be of great importance to measure the effect of the non-Markovianity of the collective dynamics on the other nuclear fission characteristics like the mean value and the dispersion of the total kinetic energy of fission fragments at infinity. This is the main purpose of the present work. We study both the saddle-to-scission time distribution and the total kinetic energy distribution in two-dimensional collective space.

The plan of the article is as follows. In Sec. II we start from the phenomenological generalized Langevin equations of motion for the collective deformation parameters. Section III is devoted to the numerical determination of the distributions of descent times and total kinetic energy of the fission fragments. Summary and conclusions are given in Sec. IV.

## II. THE MULTIDIMENSIONAL GENERALIZED LANGEVIN APPROACH TO COLLECTIVE DYNAMICS

We start our discussion of the non-Markovian aspects of nuclear large-amplitude collective motion by writing the generalized Langevin equations of motion in multidimensional collective space:

$$\begin{aligned}
 \dot{q}_i &= \sum_j B_{ij}^{-1} p_j, \\
 \dot{p}_i &= -\frac{1}{2} \sum_{jk} \frac{\partial B_{jk}^{-1}}{\partial q_i} p_j p_k - \frac{\partial E_{\text{pot}}}{\partial q_i} \\
 &\quad - \sum_{jk} \int_0^t K_{ij}(t-t', q, q') B_{jk}^{-1}(q') p_k(t') dt' + \xi_i(t), \\
 i &= 1, 2, \dots,
 \end{aligned} \tag{1}$$

\* [vkolom@kinr.kiev.ua](mailto:vkolom@kinr.kiev.ua)† [Sergey.Radionov@matfys.lth.se](mailto:Sergey.Radionov@matfys.lth.se)

which is a natural extension of one-dimensional non-Markovian Langevin dynamics given in Ref. [19] for the case of several dynamic variables. Here,  $q \equiv q_1, q_2, \dots$  stand for the collective deformation parameters and  $p \equiv p_1, p_2, \dots$  stand for the corresponding conjugate momenta,  $E_{\text{pot}}$  is the collective potential energy of deformation and  $B_{ij}$  is the inertia tensor. The noise term  $\xi_i$  in Eq. (1) is a Gaussian random process whose correlation properties are defined by the memory kernel  $K_{ij}$  of the retarded friction force through the second fluctuation-dissipation theorem [20]

$$\langle \xi_i(t) \xi_j(t') \rangle = \delta_{ij} K_{ij}(t - t', q[t], q[t']) T, \quad (2)$$

where  $T$  is temperature of a nucleus. The model (1)–(2) describes a non-Markovian Brownian motion of several collective deformation parameters in a thermal bath formed by intrinsic nucleonic degrees of freedom of a nuclear many-body system.

The memory kernel  $K_{ij}$  chosen was in the following simple form:

$$K_{ij}(t - t', q, q') = \exp\left(-\frac{|t - t'|}{\tau}\right) Z_{ij}(q, q'), \quad (3)$$

$$i, j = 1, 2, \dots,$$

where  $\tau$  is the relaxation time of collective excitations and  $Z_{ij}(q, q')$  is the non-Markovian generalization of the deformation-dependent friction tensor. The functional form of the time decay factor in Eq. (3) was dictated by our previous microscopic derivations of the time properties of collective friction given in Refs. [16,21,22]. The parameter  $\tau$  measures the strength of the memory effects in collective dynamics. Thus, in the limit of frequent collisions between nucleons,  $\tau \rightarrow 0$  (i.e., when the memory effects are relatively weak), we have a white noise process with

$$\langle \xi_i(t) \xi_j(t') \rangle \rightarrow \delta_{ij} \tau \cdot \delta(t - t') Z_{ij}(q, q) T, \quad \tau \rightarrow 0. \quad (4)$$

The retarded force in Eqs. (1) becomes a usual Markovian friction force,

$$\sum_{jk} \int_0^t K_{ij}(t - t', q, q') B_{jk}^{-1}(q') p_k(t') dt'$$

$$\rightarrow \tau \cdot \sum_j Z_{ij}(q, q) B_{jk}^{-1}(q) p_k(t), \quad \tau \rightarrow 0. \quad (5)$$

In the opposite rare collision regime,  $\tau \rightarrow \infty$ , we get a so-called blue noise with the correlation function

$$\langle \xi_i(t) \xi_j(t') \rangle \rightarrow \delta_{ij} Z_{ij}(q, q') T, \quad \tau \rightarrow \infty, \quad (6)$$

and the memory integral in Eq. (1) gives rise to a conservative force:

$$\sum_{jk} \int_0^t K_{ij}(t - t', q, q') B_{jk}^{-1}(q') p_k(t') dt'$$

$$\rightarrow \sum_{jkl} \int_{q[t=0]}^{q[t]} Z_{ij}(q, q') B_{jk}^{-1}(q') B_{kl}(q') dq'_l, \quad \tau \rightarrow \infty. \quad (7)$$

In fact, the friction in the non-Markovian system (1)–(3) is a non-monotonic function of the relaxation (memory) time  $\tau$ . It disappears both for the extremely small times  $\tau$  (when the

friction coefficient  $\sim \tau$ ) and the fairly large values of  $\tau$  (when the friction coefficient  $\sim 1/\tau$ ).

For practical applications of the model (1)–(3), we rewrite the basic equations of motion as follows

$$\dot{q}_i = \sum_j B_{ij}^{-1} p_j,$$

$$\dot{p}_i = -\frac{1}{2} \sum_{jk} \frac{\partial B_{jk}^{-1}}{\partial q_i} p_j p_k - \frac{\partial E_{\text{pot}}}{\partial q_i} - R_i(t), \quad (8)$$

$$\dot{R}_i = -\frac{R_i}{\tau} + \sum_{jk} Z_{ij}(q, q) B_{jk}^{-1}(q) p_k(t) - \alpha_i(t),$$

with  $R_i(t = 0) = 0$  and, where  $\alpha_i$  is a white Gaussian noise, with

$$\langle \alpha_i(t) \alpha_j(t') \rangle = 2\delta_{ij} Z_{ij}(q, q) T \delta(t - t'). \quad (9)$$

### III. NUMERICAL CALCULATIONS

The model (8)–(9) was applied for the study of symmetric fission of highly excited heavy nuclei. The space shape of the nuclei was obtained by rotation of some profile function  $Y^2(z)$  around the  $z$  axis. It is considered a two-parametric family of the Lorentz shapes [2]:

$$Y^2(z) = (z^2 - \zeta_0^2)(z^2 + \zeta_2^2)/Q, \quad (10)$$

where the multiplier  $Q = -\zeta_0^3(\zeta_0^2/5 + \zeta_2^2)$  guarantees the conservation of the nuclear volume. Here, all quantities of the length dimension are expressed in the radius  $R_0$  of the spherical equal-volume nucleus. The parameter  $\zeta_0$  in Eq. (10) defines an elongation of the figure, while the parameter  $\zeta_2$  is responsible for the neck of the figure. Thus, in the case of  $\zeta_2 = \infty$  we have a spheroidal shape and for  $\infty < \zeta_2 < 0$  the neck appears.

The equations of motion (8)–(9) were solved numerically with the help of the simplest Euler method with the initial conditions corresponding to the saddle-point deformation and the initial kinetic energy  $E_{\text{kin},0} = 1$  MeV (initial neck velocity  $\dot{\zeta}_2 = 0$ ). The numerical calculations were performed for the symmetric fission of a nucleus  $^{236}\text{U}$  at the temperature  $T = 2$  MeV. We define the scission line from the condition of the instability of the nuclear shape with respect to the variations of the neck radius:

$$\frac{\partial^2 E_{\text{pot}}(q)}{\partial \rho_{\text{neck}}^2} = 0, \quad (11)$$

where  $\rho_{\text{neck}} = \zeta_2 / \sqrt{\zeta_0(\zeta_0^2/5 + \zeta_2^2)}$  is the neck radius. The collective potential energies of deformation  $E_{\text{pot}}(q)$  were taken from Refs. [2] and [23]. The inertia  $B_{ij}(q)$  and friction  $Z_{ij}(q)$  tensors were determined within the hydrodynamical model [23,24].

#### A. Saddle-to-scission time distribution

First, we considered a time for the motion of a nucleus from the top of the fission barrier to the scission point (11).

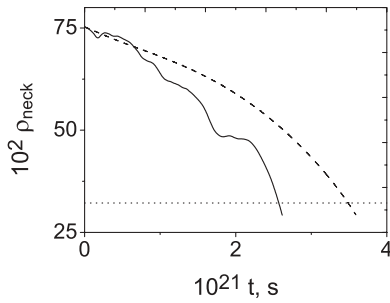


FIG. 1. Typical non-Markovian deterministic (i.e., in the absence of the random force) (dashed line) and stochastic (solid line) paths of the system (1)–(3) are shown in terms of the neck radius  $\rho_{\text{neck}}(\zeta_0, \zeta_2)$  (10) of a highly excited  $^{236}\text{U}$  for the memory time  $\tau = 2 \times 10^{-23}$  s. The horizontal line is the value of the neck radius,  $(\rho_{\text{neck}}^{\text{det}})_{\text{scis}}$ , determined from the scission condition (11) for the deterministic trajectory of the system.

Our main goal here is to measure the effect of random force on the non-Markovian dynamics (8)–(9). In practice, we used a bit different condition for the scission. Thus, we first defined the deterministic (i.e., in the absence of the stochastic force) path of the system and found the value of the neck radius of the nucleus at the scission point (11),  $(\rho_{\text{neck}}^{\text{det}})_{\text{scis}}$ . Then, we ran a total number of  $2 \times 10^4$  stochastic trajectories  $\zeta_0(t), \zeta_2(t)$  and each of them was stopped if

$$\rho_{\text{neck}}[\zeta_0(t), \zeta_2(t)] = (\rho_{\text{neck}}^{\text{det}})_{\text{scis}}. \quad (12)$$

In Fig. 1, we show a typical deterministic (dashed line) and stochastic (solid line) trajectory of the system (8)–(9) in terms of the neck radius  $\rho_{\text{neck}}(t)$ . The horizontal line in the figure is the scission value of the neck radius  $(\rho_{\text{neck}}^{\text{det}})_{\text{scis}}$ , determined from the deterministic motion of the system. A distribution  $p$  of the scission events  $t_{\text{sc}}$  at two values of the memory time  $\tau$  are computed in Fig. 2. In the first case,  $\tau_1 = 2 \times 10^{-23}$  s, the memory effects in the system are quite weak, while in the second case,  $\tau_2 = 8 \times 10^{-23}$  s, they are fairly strong. The

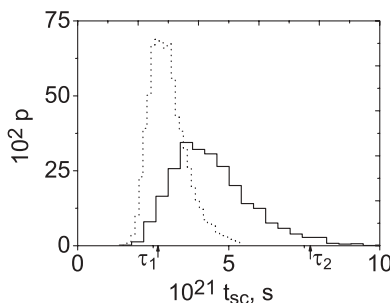


FIG. 2. A probability density histogram  $p$  of the times  $t_{\text{sc}}$  when the stochastic trajectories  $\zeta_0(t), \zeta_2(t)$  hit the scission line  $\rho_{\text{neck}}(\zeta_0, \zeta_2) = (\rho_{\text{neck}}^{\text{det}})_{\text{scis}}$ , where  $(\rho_{\text{neck}}^{\text{det}})_{\text{scis}}$  is the deterministic value of the neck radius. The dashed histogram is obtained for the memory time  $\tau_1 = 2 \times 10^{-23}$  s (when the memory effects in the system are quite weak) and the solid histogram corresponds to the memory time  $\tau_2 = 8 \times 10^{-23}$  s (when the memory effects are fairly strong). The corresponding times of descent in the absence of the random force are shown by small vertical arrows.

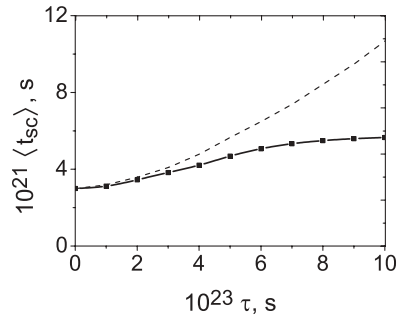


FIG. 3. The mean descent time  $\langle t_{\text{sc}} \rangle$  for the non-Markovian deterministic (dashed line) and stochastic (solid line) dynamics (1)–(3) is plotted as a function of the strength of memory effects  $\tau$ . The infinite growth of the mean time of descent for the deterministic dynamics is due to a “blocking” of the system, i.e., when the nuclear system undergoes characteristic oscillations in the vicinity of saddle point because of the additional elastic force arising from the time integral in Eq. (1) (see also Ref. [16]). In the case of non-Markovian Langevin dynamics, the mean descent time  $\langle t_{\text{sc}} \rangle$  saturates at large values of memory time  $\tau$  because the system can overcome the blocking through the thermal random jump of the collective deformation parameters  $\zeta_0, \zeta_2$  (see the Appendix).

vertical arrows in Fig. 2 represent the corresponding descent times for the deterministic motion.

We see that the descent times’ histograms  $p(t_{\text{sc}})$  are shifted to the left, compared to the deterministic estimations of the descent times  $t_{\text{sc}}$ . This fact may be explained by assuming a “stochastic acceleration” of the nuclear descent. The “acceleration” effect was earlier predicted in Ref. [18]. The scission events become more spread with the size of memory effects  $\tau$ . The fact that the non-Markovian collective dynamics occurs faster in a stochastic environment is justified by calculating the mean time of descent,  $\langle t_{\text{sc}} \rangle$ , shown in Fig. 3. The random force speeds up the nuclear motion by “shaking loose” a system and, as a consequence of that, giving rise to a smaller time of motion between two given points, compared to the corresponding time for the deterministic path of the system.

Remarkably, in the region of the small memory times  $\tau$ , the mean descent time for both the deterministic and the stochastic non-Markovian dynamics is practically the same, since at small memory times,  $\tau \rightarrow 0$ , the contribution from the random force is negligibly small [see Eq. (5) and comment to it]. In the opposite limit,  $\tau \rightarrow \infty$ , the average time of the motion from the fission barrier grows with the size of the memory effects  $\tau$ , because of the appearance of a blocking conservative force (7) preventing the nuclear descent. As seen from Fig. 3, such a blocking of the non-Markovian motion is not observed when the motion takes place in a stochastic environment and this is reflected in the saturation of the mean descent time  $\langle t_{\text{sc}} \rangle$  with  $\tau$ ; see the explanation of this fact in the Appendix.

## B. Energy distributions

We also measured the features of the non-Markovian Langevin collective dynamics by calculating a Coulomb

interaction energy at the scission,  $E_{\text{Coul}}$ , and a translation kinetic energy of the fission fragments at infinity, TKE.

The TKE is given by a sum of the mean values of the Coulomb interaction energy at the scission,  $\langle E_{\text{Coul}} \rangle$ , and the pre-scission kinetic energy  $\langle E_{\text{kin,ps}} \rangle$ ,

$$\text{TKE} = \langle E_{\text{Coul}} \rangle + \langle E_{\text{kin,ps}} \rangle. \quad (13)$$

At the scission point, the fissioning shape of the nucleus is replaced by two equal-mass spheroids for which the distance between the centers of mass,  $d$ , is the same as the distance between the two halves of the fissioning nucleus:

$$d = \frac{5}{4} \zeta_0 \frac{\zeta_0^2 + 3\zeta_2^2}{\zeta_0^2 + 5\zeta_2^2} \Big|_{\text{scis}}. \quad (14)$$

The corresponding velocity  $\dot{d}$  may be obtained by differentiation of the Eq. (14) with respect to time. The elongation  $c$  of each of the separated spheroids is defined through

$$2c + d = 2\zeta_{0,\text{scis}}, \quad (15)$$

where  $\zeta_{0,\text{scis}}$  is the scission value of the parameter  $\zeta_0$ . With the help of Eqs. (14) and (15), one can evaluate the Coulomb interaction energy  $E_{\text{Coul}}$  (see Ref. [2]) and the pre-scission kinetic energy  $E_{\text{kin,ps}}$ .

In Fig. 4, we plotted the mean value of the Coulomb interaction energy at the scission  $\langle E_{\text{Coul}} \rangle$  as a function of the memory time  $\tau$ . The corresponding deterministic calculation is shown by a dashed line. Comparing the deterministic and stochastic results for  $\langle E_{\text{Coul}} \rangle$ , one may conclude that the faster stochastic descent (see Fig. 3) leads to more compact scission configurations of the fissioning nucleus and the Coulomb interaction energy  $\langle E_{\text{Coul}} \rangle$  than in the deterministic case. As in our previous article [16], we point out that the usage of the two-spheroid parametrization (14)–(15) underestimates the value of the interaction Coulomb energy at the scission  $E_{\text{Coul}}$  on approximately 5 MeV (for the nucleus  $^{236}\text{U}$ ) obtained within more sophisticated calculations of  $E_{\text{Coul}}$  [24].

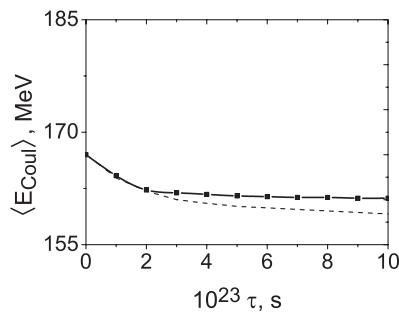


FIG. 4. The mean value of the Coulomb interaction energy of the fission fragments at the scission  $\langle E_{\text{Coul}} \rangle$  for the symmetric fission of the nucleus  $^{236}\text{U}$  at the temperature  $T = 2$  MeV. The dashed line represents the calculation of the non-Markovian dynamics in the absence of the random force. The larger values of the Coulomb energy, obtained within the non-Markovian Langevin calculation, are a result of the nuclear descent (see Fig. 3) being faster in the presence of the random force than in the absence of it. The faster a nucleus reaches a scission, the more compact its fissioning configuration is and, consequently, the larger the Coulomb interaction energy of the fission fragments at the scission  $\langle E_{\text{Coul}} \rangle$ .

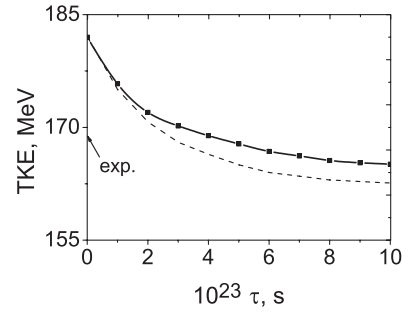


FIG. 5. The same as in Fig. 4 but for the translation kinetic energy of the fission fragments at infinity TKE (13). The arrow shows the experimental value of TKE taken from Refs. [25] and [26].

The values of the translation kinetic energy of the fission fragments at infinity are given in Fig. 5. The calculation of the TKE in the absence of the random force is plotted with a dashed line. The arrow shows the experimental value of the TKE [25,26]. In view of the last comment on Fig. 4, in the case of the deterministic motion of the system, a good agreement with the experimental data is obtained at the memory time  $\tau^{\text{det}} \approx 8 \times 10^{-23}$  s. The stochastic non-Markovian dynamics implies, at least, larger sizes of memory effects,  $\tau^{\text{stoch}} > \tau^{\text{det}}$ .

We also calculated the variance  $\sigma^2$  of the fission fragments' energy distribution. The corresponding results are presented in Fig. 6. The arrow in Fig. 6 indicates experimental data for the variance taken from Refs. [25–27]. The initial growth of the energy variance  $\sigma^2$  originates from the fact that, at small values of the memory time  $\tau$ , the time-retarded force in Eq. (1) is well approximated by usual (Markovian) friction force with the friction coefficient growing linearly with  $\tau$  [see Eq. (5)]. At large values of the memory time  $\tau$ , the friction (dissipative) part of the retarded force drops out while the conservative (time-reversible) part amplifies giving rise to the increase of the stiffness of the system. These features of the non-Markovian collective dynamics were discussed in

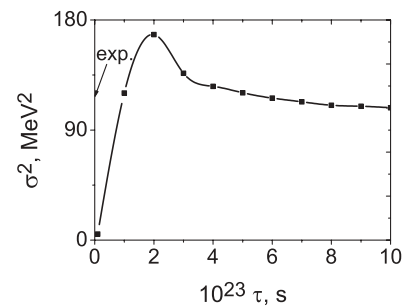


FIG. 6. The same as in Fig. 4 but for the variance  $\sigma^2$  of the translational kinetic energy distribution of the fission fragments at infinity. The experimental value of the energy variance  $\sigma^2$  [25–27] is shown by the arrow. The initial growth of the energy variance at small values of the memory time  $\tau$  is due to the fact that the time-retarded force in the equations of motion for the collective parameters (1) is reduced to the usual friction force with the friction coefficient  $\sim \tau$  at  $\tau \rightarrow 0$ . The saturation of the variance  $\sigma^2$  at large values of memory time  $\tau$  manifests the existence of the thermal fluctuations in the non-Markovian system (1)–(3) at any strength of memory effect  $\tau$  (see also Appendix).

detail for the deterministic descent from the fission barrier in Ref. [16]. Here, we found that they reveal themselves in the subsequent decrease of the variance  $\sigma^2$  of the fission fragments' energy distribution under the stochastic modeling of the nuclear descent; see the behavior of the variance at quite big strengths  $\tau$  of the memory effects in the system (1)–(3). The following fact must be pointed out. We calculated the energy variance only for the symmetric fission of  $^{236}\text{U}$ . Usually, the experimental data for the variance (as well as for the mean value) of the total kinetic energy of the fission fragments are given as an average over the variances of all observed pairs of fragments. In this respect, the value  $125 \text{ MeV}^2$  exceeds an experimentally observed value of the energy variance  $\sigma^2$  for a specific symmetric fission channel. On the other hand, the relative yield of the fission fragments with equal masses grows with the increase of the initial nuclear temperature  $T$  because of the hindrance of the shell effects. Thus, at temperatures of  $T \geq 2 \text{ MeV}$ , the fission of heavy nuclei is almost symmetric and this enables us to expect that the value  $125 \text{ MeV}^2$  relatively well reproduces the experimental value of the energy variance for the fission fragments with equal masses.

#### IV. SUMMARY AND CONCLUSIONS

The stochastic non-Markovian approach to fission dynamics based on the two-dimensional generalized Langevin equations has been used to measure the memory effects in nuclear large-amplitude collective motion. The time retardation of the friction term in the Langevin equations of motion (1) chosen was in the simple exponential form (3), where the relaxation time  $\tau$  is a parameter defining the relative size of memory effects.

The model description of the nuclear non-Markovian motion [Eqs. (1)–(3)] was applied to study the fission dynamics of a nucleus  $^{236}\text{U}$  from the top of the fission barrier to a scission (11). The collective deformation parameters were taken as parameters of the two-dimensional Lorentz family of nuclear shapes (10). By calculating the distribution of the descent times (see Figs. 2 and 3), we found that the random force accelerates significantly the descent from the barrier compared to the corresponding non-Markovian deterministic motion. The acceleration effect increases with the strength of memory effects in the system  $\tau$ . It is important to note that the mean descent time of the deterministic motion rises up monotonically with the memory time as a result of the appearance of additional conservative force from the memory integral in the equations of motion (1) (see Eq. (7) and Ref. [16]). The situation is principally different for the non-Markovian Langevin collective dynamics, i.e., when the time evolution of the nuclear deformation parameters is subject to thermal fluctuations, which leads to the saturation of the mean descent time  $\langle t_{sc} \rangle$  at fairly large values of the memory time  $\tau$  (see Fig. 3).

To investigate quantitatively the peculiarities of the non-Markovian Langevin collective motion, we calculated the first two moments of the energy distribution of the fission fragments. By comparing the calculated value of the mean kinetic energy TKE to experimental data [25,26], we estimated

the memory time and found that  $\tau^{\text{stoch}} \geq 8 \times 10^{-23} \text{ s}$ , implying the presence of fairly strong memory effects in the system [16]. The computed variance  $\sigma^2$  of the energy distribution at the value of memory time  $\tau^{\text{stoch}} \sim 8 \times 10^{-23} \text{ s}$  was found to lie relatively close to the experimentally observed variance  $\sigma_{\text{exp}}^2 \approx 125 \text{ MeV}^2$  [25–27] (see Fig. 6 and our comment on the experimental determination of the variance  $\sigma^2$  for symmetric fission of heavy nuclei).

#### APPENDIX

To demonstrate the presence of the thermal fluctuations in the collective dynamics (8)–(3) in the regime of infinitely strong memory effects,  $\tau \rightarrow \infty$ , we start from a schematic one-dimensional description of large-amplitude collective motion as was done in Ref. [28]. We introduce a single collective deformation parameter  $q$  and write a linearized Langevin equation of motion for  $q$  in the following form:

$$B\dot{q} = k(q - q_0) - \bar{k} \int_0^t \exp\left(-\frac{|t-t'|}{\tau}\right) \dot{q}(t') dt' + \xi(t), \quad (\text{A1})$$

where  $q_0$  is the initial value of the collective parameter,  $k$  is the drift coefficient,  $\bar{k}$  is the model coefficient, and  $\xi(t)$  is the Ornstein-Uhlenbeck stochastic process with the correlation function

$$\langle \xi(t)\xi(t') \rangle = T\bar{k} \exp\left(-\frac{|t-t'|}{\tau}\right). \quad (\text{A2})$$

The model description (A1) of the nuclear collective motion allows us to have an analytical solution close to the time evolution of the collective parameter  $q$  [28],

$$q(t) = q_0 + B(t)v_0 + \int_0^t B(t-t')\xi(t') dt', \quad (\text{A3})$$

with

$$B(t) = C_\kappa e^{\kappa t} + A_\omega e^{-\gamma t} \sin(\omega t) + B_\omega e^{-\gamma t} \cos(\omega t). \quad (\text{A4})$$

Here, the constants  $A_\omega$ ,  $B_\omega$ , and  $C_\kappa$  are given by

$$C_\kappa = \frac{\kappa + a}{(\kappa + \gamma)^2 + \omega^2}, \quad A_\omega = -\frac{(\kappa + \gamma)(-\gamma + a) - \omega^2}{\omega[(\kappa + \gamma)^2 + \omega^2]},$$

$$B_\omega = -\frac{\kappa + a}{(\kappa + \gamma)^2 + \omega^2}, \quad (\text{A5})$$

where

$$\kappa = A_1 + B_1 - a/3, \quad \gamma = (A_1 + B_1)/2 + a/3,$$

$$\omega = \sqrt{3}(A_1 - B_1)/2,$$

with

$$A_1 = [ -((a/3)^3 - ab/6 + c/2) + \sqrt{((-a^2/9 + b/3)^3 + ((a/3)^3 - ab/6 + c/2)^2)} ]^{1/3},$$

$$B_1 = [ -((a/3)^3 - ab/6 + c/2) - \sqrt{((-a^2/9 + b/3)^3 + ((a/3)^3 - ab/6 + c/2)^2)} ]^{1/3},$$

and

$$a = 1/\tau, \quad b = -k + \bar{k}, \quad c = -k/\tau.$$

The parameter  $\kappa$  determines the drift of the system from the top of the fission barrier,  $\gamma$  and  $\omega$  define, correspondingly, the damping and frequency of the characteristic shape oscillations of a nucleus appearing at fairly large values of memory time  $\tau$  (see Ref. [16]). With the growth of memory effects, the system in the absence of the stochastic term in Eq. (A1) becomes more and more blocked because of the additional elastic force appearing from the time integral. In the limit  $\tau \rightarrow \infty$ , the system undergoes pure ( $\kappa = 0$ ) undamped ( $\gamma = 0$ ) oscillations given by

$$q^{\text{det}}(t) = q_0 + \frac{\sin(\omega t)}{\omega} \cdot v_0. \quad (\text{A6})$$

The amplitude of these oscillations is quite small such that the system is blocked and can not reach a scission point,  $q^{\text{det}}(t) \ll q_{\text{scis}}$ .

If the collective dynamics is affected by the random force, described in terms of the Ornstein-Uhlenbeck process (A1) and (A2), the thermal fluctuation part,  $q^{\text{stoch}}$ , always presents in the collective deformation's time evolution even in the limit of infinitely strong memory effects,  $\tau \rightarrow \infty$ ,

$$q^{\text{stoch}} = \frac{1}{\omega} \int_0^t \sin(\omega(t-t')) \xi(t') dt'. \quad (\text{A7})$$

Therefore, one can claim that the non-Markovian stochastic dynamics (A1) and (A2) provides reaching of the scission for finite times at any size of memory effects  $\tau$ . This feature of the generalized Langevin motion shows up in the saturation of the mean descent times  $\langle t_{\text{sc}} \rangle$  at the large values of memory times  $\tau$  seen in Fig. 3. Also, this feature would imply nonzero values of the dispersions of dynamical variables as can be seen from Fig. 6 for the variance of the energy distribution of fission fragments.

- 
- [1] P. J. Siemens and A. S. Jensen, *Elements of Nuclei: Many-Body Physics with the Strong Interaction* (Addison-Wesley, Reading, MA, 1987).
- [2] R. W. Hasse and W. D. Myers, *Geometrical Relationships of Macroscopic Nuclear Physics* (Springer-Verlag, Berlin/Heidelberg, 1988).
- [3] H. Hofmann, Phys. Rep. **284**, 137 (1997).
- [4] R. Balescu, *Equilibrium and Nonequilibrium Statistical Mechanics* (Wiley, New York, 1975), Vol. 2.
- [5] D. Boilley, E. Suraud, Y. Abe, and S. Ayik, Nucl. Phys. **A556**, 67 (1993).
- [6] D. Boilley, Y. Abe, S. Ayik, and E. Suraud, Z. Phys. A **349**, 119 (1994).
- [7] Y. Abe, S. Ayik, P.-G. Reinhard, and E. Suraud, Phys. Rep. **275**, 49 (1996).
- [8] J. Frenkel, *Kinetic Theory of Liquids* (Clarendon, Oxford, 1946).
- [9] S. Ayik and W. Nörenberg, Z. Phys. A **309**, 121 (1982).
- [10] K. Niita, W. Nörenberg, and S. J. Wang, Z. Phys. A **326**, 69 (1987).
- [11] V. M. Kolomietz, Phys. Rev. C **52**, 697 (1995).
- [12] H. Hofmann and D. Kiderlen, Phys. Rev. C **56**, 1025 (1997).
- [13] V. M. Kolomietz, *Local Density Approach for Atomic and Nuclear Physics* (Naukova Dumka, Kiev, 1990) (in Russian).
- [14] D. Kiderlen, V. M. Kolomietz, and S. Shlomo, Nucl. Phys. **A608**, 32 (1996).
- [15] V. M. Kolomietz and S. Shlomo, Phys. Rep. **390**, 133 (2004).
- [16] V. M. Kolomietz, S. V. Radionov, and S. Shlomo, Phys. Rev. C **64**, 054302 (2001).
- [17] A. E. Gegechkori, Yu. A. Anischenko, P. N. Nadochay, and G. D. Adeev, Yad. Fiz. **71**, 2041 (2009).
- [18] D. Boilley and Y. Lallouet, J. Stat. Phys. **125**, 473 (2006).
- [19] S. A. Adelman, J. Chem. Phys. **64**, 124 (1976).
- [20] R. Kubo, Rep. Prog. Phys. **29**, 255 (1966).
- [21] S. Radionov and S. Åberg, Phys. Rev. C **71**, 064304 (2005).
- [22] V. M. Kolomietz, S. Åberg, and S. V. Radionov, Phys. Rev. C **77**, 014305 (2008).
- [23] W. D. Myers and W. J. Swiatecki, Ark. Fys. **36**, 343 (1967).
- [24] K. T. R. Davies, R. A. Managan, J. R. Nix, and A. J. Sierk, Phys. Rev. C **16**, 1890 (1977).
- [25] M. G. Itkis and A. Ya. Rusanov, Part. Nucl. **29**, 390 (1998).
- [26] G. D. Adeev and V. V. Pashkevich, Nucl. Phys. **A502**, 405c (1989).
- [27] Yu. A. Lazarev, At. Energy Rev. **15**, 75 (1977).
- [28] V. M. Kolomietz, S. V. Radionov, and S. Shlomo, Phys. Scr. **73**, 458 (2006).